Deficient ryanodine receptor *S*-nitrosylation increases sarcoplasmic reticulum calcium leak and arrhythmogenesis in cardiomyocytes

Daniel R. Gonzalez, Farideh Beigi, Adriana V. Treuer, and Joshua M. Hare*

Department of Medicine, Cardiovascular Division, and Interdisciplinary Stem Cell Institute, Miller School of Medicine, University of Miami, 1120 Northwest 14th Street, Suite 1124, Miami, FL 33136

Edited by Solomon H. Snyder, Johns Hopkins University School of Medicine, Baltimore, MD, and approved October 29, 2007 (received for review July 23, 2007)

Altered Ca^{2+} homeostasis is a salient feature of heart disease, where the calcium release channel ryanodine receptor (RyR) plays a major role. Accumulating data support the notion that neuronal nitric oxide synthase (NOS1) regulates the cardiac RyR via *S*-nitrosylation. We tested the hypothesis that NOS1 deficiency impairs RyR *S*-nitrosylation, leading to altered Ca^{2+} homeostasis. Diastolic Ca^{2+} levels are elevated in NOS1$^{-/-}$ and NOS1/NOS3$^{-/-}$ but not NOS3$^{-/-}$ myocytes compared with wild-type (WT), suggesting diastolic Ca^{2+} leakage. Measured leak was increased in NOS1$^{-/-}$ and NOS1/NOS3$^{-/-}$ but not in NOS3$^{-/-}$ myocytes compared with WT. Importantly, NOS1$^{-/-}$ and NOS1/NOS3$^{-/-}$ myocytes also exhibited spontaneous calcium waves. Whereas the stoichiometry and binding of FK-binding protein 12.6 to RyR and the degree of RyR phosphorylation were not altered in NOS1$^{-/-}$ hearts, RyR2 *S*-nitrosylation was substantially decreased, and the level of thiol oxidation increased. Together, these findings demonstrate that NOS1 deficiency causes RyR2 hyponitrosylation, leading to diastolic Ca^{2+} leak and a proarrhythmic phenotype. NOS1 dysregulation may be a proximate cause of key phenotypes associated with heart disease.

heart | nitric oxide | excitation–contraction coupling | oxidative stress | heart failure

The cardiac myocyte has emerged as a prototypic example of the manner in which nitric oxide (NO) signaling occurs in a spatially confined manner. Although neuronal (NOS1) and endothelial (NOS3) isoforms of nitric oxide synthase are located extremely close to one another within the cell on opposite sides of the dyad, they exert opposite effects on myocardial contractility (1). The mechanism(s) for this effect remains controversial. One explanation derived from *in vitro* observations is that NOS3 inhibits the sarcolemmal L-type calcium channel on the sarcolemmal aspect of the dyad, whereas NOS1 modulates ryanodine receptor (RyR) activity on the sarcoplasmic reticulum (SR) (1–3). Although this paradigm explains many facets of NO activity within the heart, other studies suggest that in the myocyte, NOS1 may bind to and/or regulate other ion channels or effectors, including the plasma membrane calcium/calmodulin-dependent calcium ATPase (4), sarcoplamic reticulum Ca^{2+}-ATPase (SERCA) (5), and possibly phospholamban (PLB). In addition, there is support for the notion that this effect is mediated by a direct protein posttranslational modification; but again, this assertion is controversial (6).

Another facet of NO cardiobiology has emerged that further motivates the importance of understanding the direct NOS effector molecules. In heart failure and/or other states of cardiac injury, NOS1 levels within the heart rise, and NOS1 effectively translocates from the SR to the plasma membrane (2, 7, 8). Because this phenomenon could have either deleterious effects or adaptive consequences, it is imperative to address definitively the physiologic role of NOS1 in the heart.

To address these issues, we tested the hypothesis that the cardiac RyR is a primary target for NO physiologic modulation. We predicted that the described protein–protein interaction between NOS1 and the RyR2 facilitates highly specific modulation of this channel via *S*-nitrosylation. For this purpose, we studied the calcium homeostasis of cardiac myocytes from wild-type (WT) mice and those lacking one or both constitutive NOS isoforms. We found that lack of NOS1 altered RyR behavior associated with decreased *S*-nitrosylation and increased oxidation of the channel, producing diastolic Ca^{2+} leak with a negative impact in cardiac electrical stability and contractility.

Results

Force–Frequency Relationship and Diastolic Intracellular Ca^{2+} Concentration ($[Ca^{2+}]_i$). As we have previously described (9, 10), the force–frequency relationship is depressed in NOS1$^{-/-}$ mice. Consistent with these observations, when field-stimulated at 2, 4, 6, and 8 Hz, the degree of sarcomere shortening and the amplitude of calcium transients in cardiomyocytes (Fig. 1 *a* and *b*) were significantly reduced in NOS1$^{-/-}$ and NOS1/NOS3$^{-/-}$ compared with both WT and NOS3$^{-/-}$ myocytes (9, 10).

Because reduced Ca^{2+} transients could be the result of either RyR dysfunction or impaired Ca^{2+} reuptake into the SR, we measured systolic and diastolic levels of $[Ca^{2+}]_i$ in the four strains of mice. We first noted that diastolic Ca^{2+} levels rose over the full range of stimulation frequencies in NOS1$^{-/-}$ and NOS3/NOS1$^{-/-}$ but not in NOS3$^{-/-}$ myocytes (Fig. 1*c*), a finding suggestive of a diastolic Ca^{2+} leak or defective Ca^{2+} reuptake. Conversely, we found that parameters of Ca^{2+} reuptake, τ, and TR50 (time to achieve 50% of decay) were not different among WT, NOS1$^{-/-}$, NOS3$^{-/-}$, and NOS1/NOS3$^{-/-}$ myocytes, suggesting that SR calcium reuptake function (mediated by SERCA2) is not responsible for the observed abnormalities in Ca^{2+} handling in NOS1$^{-/-}$ (Fig. 1*d*). Additionally, Na/Ca exchanger (NCX) function was not apparently different between WT and NOS1$^{-/-}$ myocytes (Fig. 1*e*). These results support the hypothesis that a diastolic Ca^{2+} leak from the SR may be the underlying cause of the altered Ca^{2+} handling in NOS1-deficient mice.

Assessment of SR Ca^{2+} Content and Diastolic Ca^{2+} Leakage. To address this possibility, we directly measured SR Ca^{2+} leak by using an established protocol (11) (Fig. 2*a*). As shown, NOS1 deficiency is also associated with reduced SR Ca^{2+} content compared with WT, whereas at 4 Hz it was increased in NOS3$^{-/-}$ myocytes (Fig. 2*b*). NOS1$^{-/-}$ and NOS1/NOS3$^{-/-}$ myocytes exhibited substan-

Author contributions: D.R.G. and J.M.H. designed research; D.R.G., F.B., and A.V.T. performed research; D.R.G. and J.M.H. analyzed data; D.R.G. and J.M.H. wrote the paper.

The authors declare no conflict of interest.

This article is a PNAS Direct Submission.

*To whom correspondence should be addressed. E-mail: jhare@med.miami.edu.

This article contains supporting information online at www.pnas.org/cgi/content/full/0706796104/DC1.

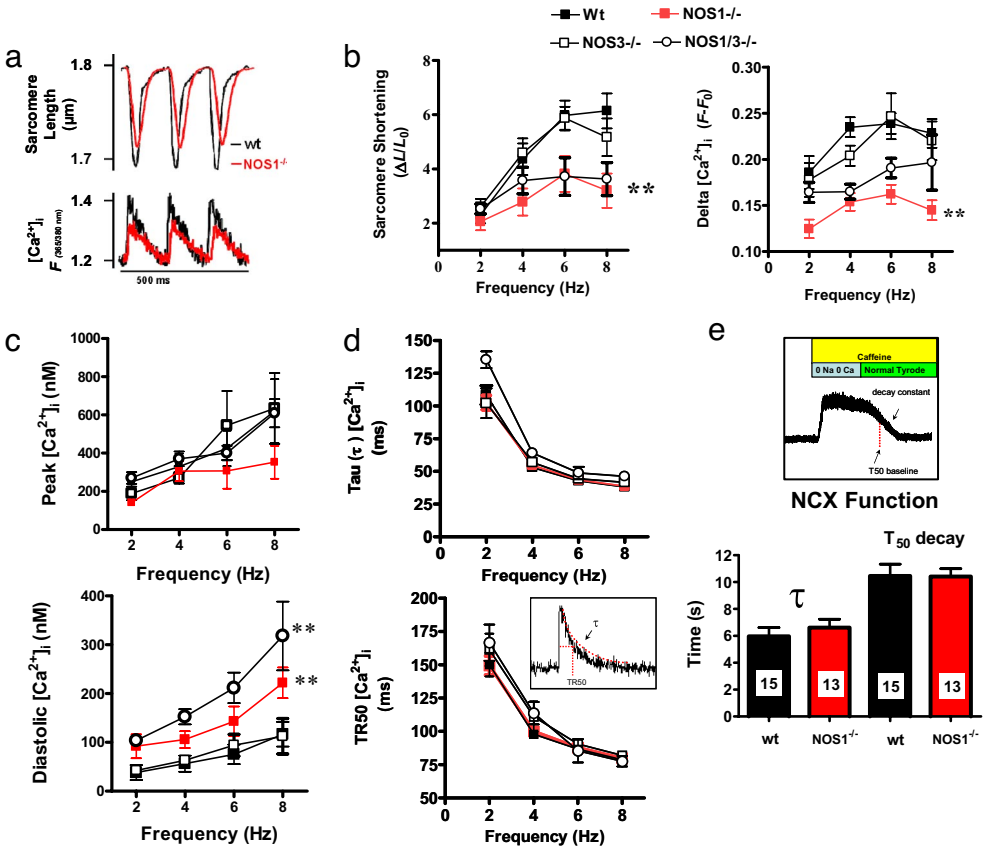

Fig. 1. Force–frequency relationship and parameters of Ca^{2+} removal. (*a*) Representative traces of sarcomere shortening and calcium transients ($[Ca^{2+}]_i$) for wild-type (wt) and NOS1-deficient myocytes. (*b*) Sarcomere shortening and the amplitude of $[Ca^{2+}]_i$ transients ($F - F_0$) in response to increased frequency of stimulation is impaired in NOS1$^{-/-}$ and NOS1/NOS3$^{-/-}$ but not in NOS3$^{-/-}$ myocytes. **, $P < 0.05$ vs. WT and NOS3$^{-/-}$. (*c*) Calibrated values of systolic (peak) and diastolic $[Ca^{2+}]_i$. NOS1$^{-/-}$ and NOS1/NOS3$^{-/-}$ myocytes showed increased diastolic levels of $[Ca^{2+}]_i$. **, $P < 0.05$ vs. WT and NOS3$^{-/-}$. (*d*) Frequency-dependent acceleration of $[Ca^{2+}]_i$ decay was estimated as a constant of decay (τ) and TR50 (time to reach 50% of baseline values). Both parameters were not significantly different among strains. (*e*) NCX function. Tau and T_{50} were used to analyze the function of the sodium calcium exchanger NCX during a pulse of caffeine superfusion.

tially increased leak for a given Ca^{2+} load compared with WT (Fig. 2*c*). Importantly, the fractional Ca^{2+} release was increased in NOS1$^{-/-}$ cardiomyocytes, denoting increased sensitivity of RyR to luminal Ca^{2+} (Fig. 2*d*).

This protocol revealed another important phenotype shown to be associated with myocyte electrical instability. During the period of 0 Na^+/0 Ca^{2+} treatment, both NOS1$^{-/-}$ and NOS1/NOS3$^{-/-}$ myocytes displayed spontaneous Ca^{2+} transients (Fig. 3 *a* and b). These transients were most probably caused by RyR2 opening because they were abolished by tetracaine treatment and they occurred in the absence of extracellular Na^+ or Ca^{2+}, which impairs NCX activity.

Additionally, we exposed WT and NOS1$^{-/-}$ myocytes (paced at 1 Hz) to high extracellular calcium. To do so, the extracellular concentration was increased from 1.8 to 5 mM ($[Ca^{2+}]_o$) to test SR capacity to handle high Ca^{2+} load (12). In WT myocytes (Fig. 3*d*), this maneuver increased the amplitude of the Ca^{2+} transient, without signs of Ca^{2+} disturbances ($n = 4$ cells). On the contrary,

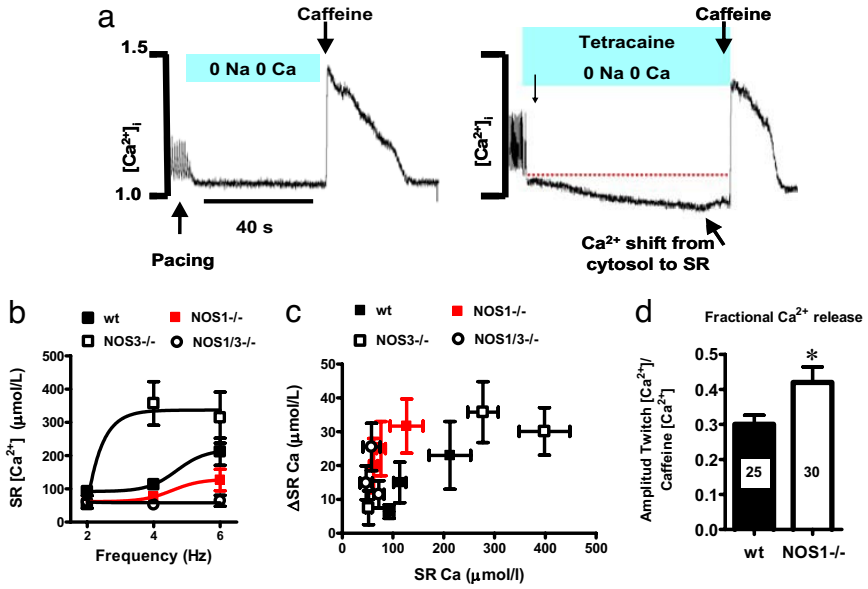

Fig. 2. Assessment of SR calcium leak and load–leak relationship. (*a*) Representative tracings showing the protocol for Ca^{2+} leak. After stimulating the myocytes (4 Hz in the example), the solution is changed to a Na^+/Ca^{2+}-free (0 Na^+/0 Ca^{2+}) medium for 40 s. After a period of recovery, the cells are challenged again at the same frequency, with the Na/Ca-free medium containing 1 mM tetracaine, a RyR blocker. The decrease in the signal of fura corresponds to the Ca^{2+} leak. (*b*) Intra-SR Ca^{2+} content as a function of frequency of stimulation. The increased frequencies induce increase in the Ca^{2+} load. (*c*) Shift in intra-SR Ca^{2+} content (change in cytosolic Ca^{2+} with tetracaine) as a function of the load. Despite a decreased load of Ca^{2+} into the SR, the tetracaine-induced shift is increased in NOS1$^{-/-}$ and NOS1/3$^{-/-}$ myocytes compared with the wild type (wt), suggesting increased diastolic leak. (*d*) Fractional release of Ca^{2+} after stimulation of the cells at 4 Hz and a pulse of 10 mM caffeine (the number of myocytes studied appears inside the bar; *, $P < 0.05$ vs. WT.

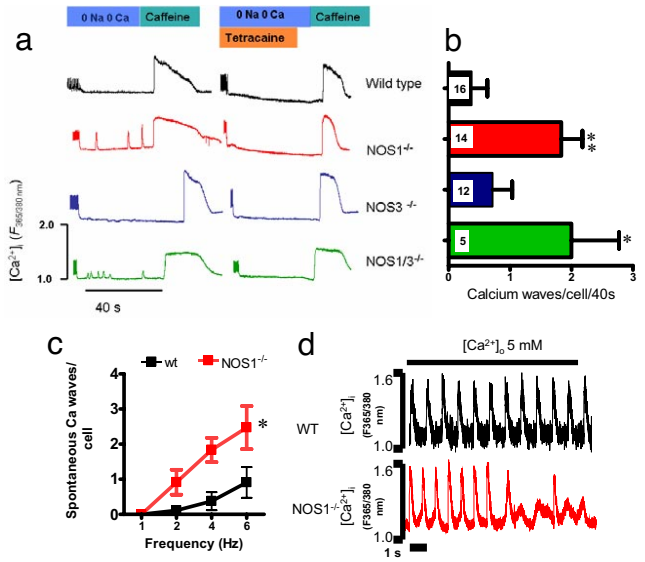

Fig. 3. Arrythmogenic Ca^{2+} waves in NOS1-deficient myocytes. (*a*) Representative traces of WT, NOS1$^{-/-}$, NOS1/NOS3$^{-/-}$, and NOS3$^{-/-}$ myocytes stimulated at 4 Hz. After a pause in 0 Na^+/0 Ca^{2+} buffer, intracellular Ca^{2+} waves appeared in NOS1$^{-/-}$ and NOS3/NOS1$^{-/-}$ cells. They were abolished with the presence of tetracaine. (*b*) Quantification of spontaneous Ca^{2+} waves per cell displayed by WT, NOS1$^{-/-}$, NOS3$^{-/-}$, and NOS1/3$^{-/-}$ cardiomyocytes stimulated at 4 Hz; *, $P < 0.05$; **, $P < 0.01$ vs. WT. (*c*) Analysis of spontaneous Ca^{2+} waves displayed by WT, NOS1$^{-/-}$ cardiomyocytes stimulated from 1 to 6 Hz. *, $P < 0.05$ vs. WT. (*d*) Impact of high extracellular Ca^{2+} concentration on Ca^{2+} waves. WT and NOS1$^{-/-}$ myocytes were switched from 1.8 mM extracellular calcium to 5 mM. NOS1$^{-/-}$ displayed diastolic Ca^{2+} waves (four of five cells) but not WT myocytes (zero of four).

in NOS1$^{-/-}$ myocytes, Ca^{2+} waves were observed (four of five cells). This result suggests that in NOS1$^{-/-}$ myocytes, the calcium release channel RyR2 exhibits increased sensitivity to luminal Ca^{2+}.

To test the possibility that increased RyR activity is able to produce significant diastolic leak and that leak is relevant at higher rates of stimulation, we treated WT myocytes with 0.5 mM and 1 mM caffeine, concentrations that increase RyR open probability without depleting the SR (12). We stimulated the cells at 0.5 and 4 Hz and applied caffeine. Caffeine showed only a transient effect when cells were paced at 0.5 Hz. On the contrary, at 4 Hz, caffeine increased the diastolic $[Ca^{2+}]_i$ and decreased the peak of $[Ca^{2+}]_I$ [see supporting information (SI) Fig. 7].

Next, we tested whether pharmacological inhibition of NOS1 with 1 μM *S*-methylthiocitrulline, a specific NOS1 inhibitor (13), mimics the effects of the genetic deletion. This maneuver produced a decrease in the SR Ca^{2+} content and induced the appearance of Ca^{2+} waves (Fig. 4). To reverse this phenotype, we treated NOS1$^{-/-}$ myocytes with a NO donor. The cells were incubated with 100 μM diethylenetriamine/NO (DETA/NO) for 5 min and after this period, paced at 4 Hz for the leakage protocol. DETA/NO increased SR content but did not reduce the diastolic Ca^{2+} waves (Fig. 4*b*).

RyR2 Phosphorylation and Binding to FKBP12.6. We examined whether NOS1 disruption and the resulting Ca^{2+} leak were associated with alterations in the abundance of SR Ca^{2+}-handling proteins. Western blot analysis revealed that RyR2 expression is increased in the NOS1$^{-/-}$ hearts (Fig. 5*a*), as reported (14). Also, we performed coimmunoprecipitation experiments to study the stoichiometry of FK-binding protein 12.6 (FKBP12.6): RyR2. There was no significant difference in the amount of FKBP12.6 bound to RyR2 in both strains (Fig. 5*b*).

Because RyR2 phosphorylation alters the channel activity and binding to FKBP12.6 (15, 16), we further investigated its phosphorylation status in WT and NOS1$^{-/-}$ animals by using a specific antibody against phosphorylated Ser-2809 (Fig. 5*c*). The ratio of phosphorylated RyR to total RyR was not different between both groups ($n = 6$). Additionally, we studied the levels of other proteins involved in Ca^{2+} handling by Western blot analysis. We found no significant changes in calsequestrin, PLB, L-type calcium channel, or SERCA2a. Only NCX was significantly up-regulated (data not shown), although in our hands its activity remained unchanged, probably because of the competition with other systems such as the sarcolemmal calcium ATPase and mitochondrial uniporter (17).

***S*-Nitrosylation and Oxidation of RyR2.** We evaluated the degree of *S*-nitrosylation of RyR2 because this modification has been shown in electrophysiological experiments to alter the open probability of the channel. For this purpose, we performed the biotin switch coupled to immunoprecipitation of RyR2 (Fig. 6*a*). With this assay, we found decreased *S*-nitrosylation of RyR2 in NOS1$^{-/-}$ mice compared with WT and NOS3$^{-/-}$. We further confirmed this result by submitting a different set of hearts to the biotin switch, with a technique of selective isolation of biotinylated proteins with streptavidin-agarose (SI Fig. 8). This method showed near absence of RyR2 *S*-nitrosylation in NOS1$^{-/-}$ hearts. As a control, we also analyzed GAPDH, a well known *S*-nitrosylated protein (see SI Fig. 8). It was equally nitrosylated in both strains, highlighting the

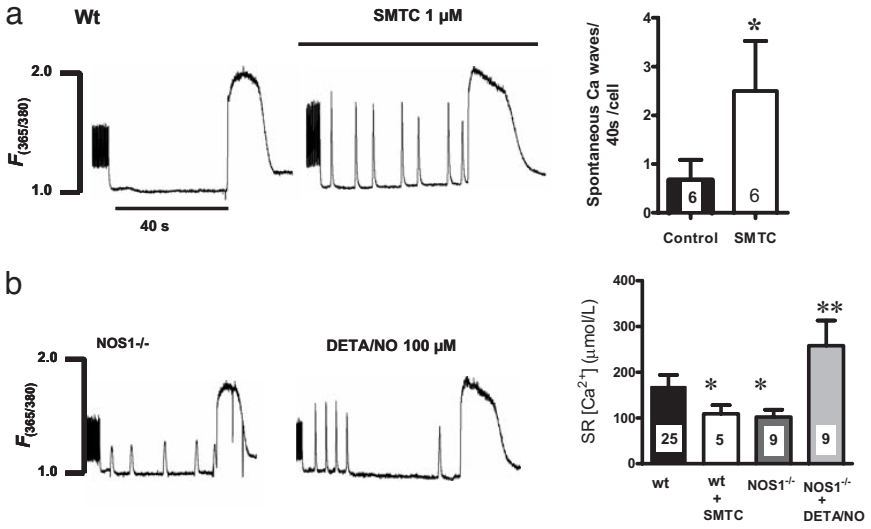

Fig. 4. Fig. 4. Pharmacological manipulations with NOS1 blocker and NO donor. (*a*) Wild-type myocytes (Wt) were treated with the specific NOS1 inhibitor *S*-methylthiocitrulline (SMTC; 1 μM). After 15 min, the cells were challenged with the Na^+/Ca^{2+}-free buffer and after 40 s, with a pulse of caffeine. (*b*) NOS1$^{-/-}$ cells were treated with an NO donor (DETA/NO, 100 μM) and then challenged with the Na^+/Ca^{2+}-free solution and caffeine to assess intra-SR Ca^{2+} content (*, $P < 0.05$ vs. WT; **, $P < 0.01$ vs. WT and NOS1$^{-/-}$; the number of myocytes appears inside the bar).

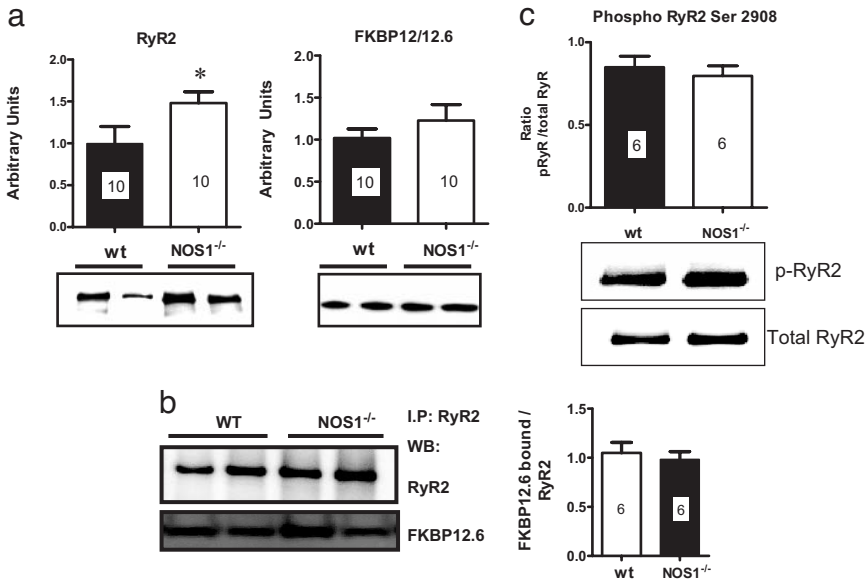

Fig. 5. Stoichiometry of FKBP12.6 binding to and phosphorylation of RyR2. (*a*) Western blots of RyR2 and FKBP12/12.6. Heart homogenates of wild-type (wt) and NOS1$^{-/-}$ mice ($n = 10$) were analyzed for total content of RyR2 and total FKBP12/12.6. ⋆, $P < 0.05$ vs. WT. (*b*) The specific binding of FKBP12.6 to RyR2 was further analyzed by coimmunoprecipitation in both strains with an anti-RyR2 antibody ($n = 6$). (*c*) Phosphorylation status of RyR was also measured by using a specific antibody against the phosphorylated Ser-2908 and compared with the total amount of RyR2. The number of myocytes is depicted in each bar.

importance of the subcellular localization for the regulation of nitrosylation. In addition, RyR nitrosylation was not altered in hearts of NOS3$^{-/-}$ mice.

We also assessed the relative free thiol content of the RyR2 in WT, NOS1$^{-/-}$, and NOS3$^{-/-}$ mice hearts with monobromobimane (mBB), a specific probe for free cysteines (not nitrosylated, disulfide bonds or higher oxidized forms). We found that the mBB signal was decreased in NOS1$^{-/-}$ hearts compared with WT and NOS3$^{-/-}$ (Fig. 6*b* and SI Fig. 9), consistent with increased oxidation. Given this result and decreased *S*-nitrosylation levels, we infer that in NOS1$^{-/-}$ hearts there is an increased degree of cysteine oxidation of RyR2

Discussion

The major finding of the present work is that NOS1 is responsible for endogenous nitrosylation of the cardiac ryanodine receptor. RyR2 from NOS1-deficient mice is hyponitrosylated, and excitation–contraction coupling in these myocytes is marked by diastolic Ca^{2+} leak. Importantly, this leakage causes not only depressed cardiac contractile reserve but also proarrhythmic spontaneous Ca^{2+} waves, which have been associated with sudden cardiac death (18). These findings demonstrate the endogenous regulation of the RyR2 by a specific NOS isoform and offer insights into the pathophysiology of cardiac injury and arrhythmias.

It is demonstrated in lipid bilayer preparations that both RyR1 (19–22) and RyR2 (3) are nitrosylated at specific cysteine residues. In separate lines of work, several groups, including our own, have demonstrated the presence of NOS1 in the cardiac SR in proximity to RyR2 (5, 23, 24). Recently, it has been shown that increasing the frequency of stimulation activates NO production from NOS1, in a calmodulin-dependent manner (25). Whether or not NOS1 is required for endogenous RyR2 nitrosylation and the linkage of it to cellular pathophysiology was heretofore unknown. The present results establish that indeed NOS1 but not NOS3 is the NOS isoform required for RyR2 nitrosylation and that NOS1 deficiency causes two key pathophysiologic features: diastolic Ca^{2+} leak and spontaneous diastolic Ca^{2+} waves.

The characteristics we have found in the NOS1$^{-/-}$ phenotype resemble those observed in certain mutations of RyR (26) that

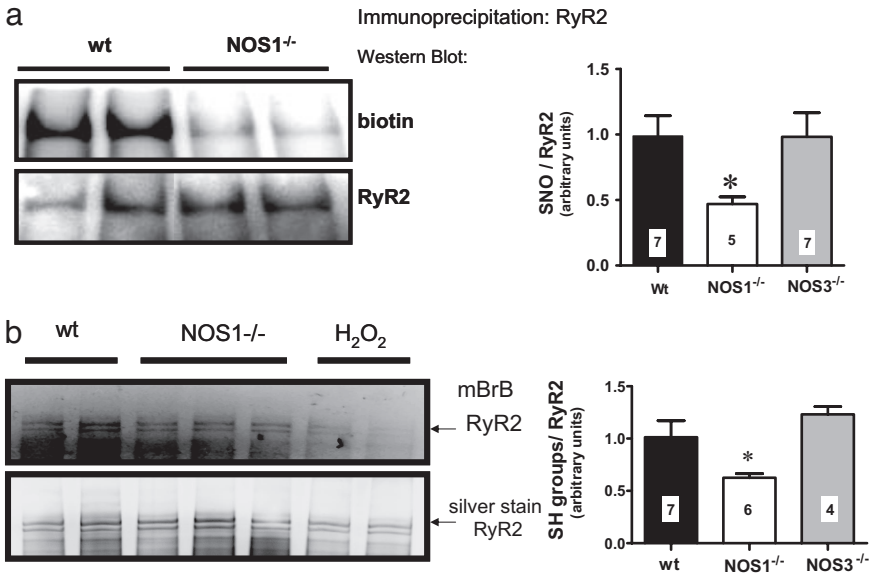

Fig. 6. Analysis of RyR2 *S*-nitrosylation and free cysteines. (*a*) RyR *S*-nitrosylation assessed by the biotin switch. Hearts of wild-type (wt) and NOS1$^{-/-}$ mice were submitted to the biotin switch and immunoprecipitated with anti-RyR2 antibody. (*Upper*) Representative Western blot using an anti-biotin antibody. (*Lower*) Total RyR2 in the samples. The bar graph resumes the ratio of the biotin signal to the total RyR2 (no. of samples indicated in bar graph; ⋆, $P < 0.05$ vs. WT and NOS3$^{-/-}$, ANOVA). (*b*) Assessment of free cysteines in RyR2. Heart homogenates were labeled with monobromobimane (mBrB), a specific probe for free cysteines. Then the samples were resolved by electrophoresis and the free cysteines were visualized by UV light transillumination. (*Upper*) Intensity of free cysteines in wild-type and NOS1$^{-/-}$ homogenates. As a control, wild-type hearts were perfused with 1 and 10 mM H_2O_2, respectively. (*Lower*) Total content of RyR by silver staining of the gels (no. of samples indicted in bar graph; ⋆, $P < 0.05$ vs. WT and NOS3$^{-/-}$, ANOVA).

include cysteine residues (27) and also in the phenotype of calsequestrin- (28), junctin- (29), and FKBP12.6-deficient mice (30). The cardiomyocytes of these animals display diastolic Ca^{2+} leak, spontaneous SR Ca^{2+} release, triggered beats, and increased mortality.

Several lines of evidence implicate a role for oxidative stress in the modulation of RyR2 activity. In NOS1-deficient mice, we and others have reported an increase in reactive oxygen species (10, 31), and it is reasonable to infer that oxidative stress may oxidize reactive thiols on RyR2. Indeed, we demonstrate a decreased number of free cysteines in $NOS1^{-/-}$ hearts, which, along with the decreased *S*-nitrosylation, suggests oxidation of the channel. It is known that NOS1 deficiency can augment ROS generation from xanthine oxidase (10), further supporting a model of NO/redox imbalance in this mouse.

In this context, the observation that exogenous NO application (100 μM DETA/NO) was unable to prevent Ca^{2+} waves completely suggests the possibility of irreversible oxidation of some cysteines. Indeed, it has been described that further oxidation of cysteines is involved in irreversible activation of RyR2 (3). Another possibility is that low-molecular weight *S*-nitrosothiols such as *S*-nitrosoglutathione or nitrosocysteine, which are more physiological, could be able to restore the redox state of the channel instead of DETA/NO.

In a canine model of heart failure, an increase in RyR oxidation and Ca^{2+} leak was observed and corrected by antioxidant treatment (32). In this sense, *S*-nitrosylation may prevent oxidation of reactive thiols of the channel, which is known to induce cross-linking between the subunits of RyR and increase the open probability of the channel, and NO is able to prevent this modification (33). In the canine heart, RyR2 is endogenously *S*-nitrosylated, with a stoichiometry of 1 *S*NO per RyR subunit (3) and in a manner that is competitive with thiol oxidation (33). In this way, NOS1-derived nitrosylation may control the basal redox state of the channel. In the case of heart failure, with increased oxidative stress, multiple thiols may be involved in oxidation. Furthermore, it has been suggested that the tonic NO production in the SR may keep RyR in the closed state (34), which has also been observed with some NO donors (35, 36). Recently, also in a canine model of heart failure, decreased intra-SR Ca^{2+} content, associated with increased Ca^{2+} leak via RyR2, was observed (37). Importantly, these authors found an increased sensitivity of RyR to intraluminal Ca^{2+} concentrations. In other words, even when the SR Ca^{2+} content is decreased, the gating of RyR at lower luminal Ca^{2+} concentrations is increased, favoring the conditions for leak. We observed this behavior in $NOS1^{-/-}$ myocytes: an increased Ca^{2+} sensitivity and a partial depletion of the SR, along with increased leak.

Whereas with physiological muscle activity, *S*-nitrosylation of the RyR may produces reversible activation (required, for instance, during β-adrenergic activation), in the pathological state, chronic RyR oxidation increases RyR open probability in a more sustained, less reversible manner (3, 38). Also, it has been shown in preparations of RyR2 reconstituted in lipid bilayers that oxidation of the channel shifts the relationship between pCa and open probability of the channel to the left (38), denoting increased sensitivity to activating calcium, a feature that is compatible with our observations. On the contrary, exogenous NO at physiological O_2 tension inhibits the activity of RyR1 at high $[Ca^{2+}]$ (20).

Chronic diastolic leak leads to partial depletion of the SR (37) and increases the predisposition to ventricular arrhythmias and sudden death (30). We have described premature death in NOS1- and NOS1/$NOS3^{-/-}$-deficient mice (39) and recently, in a model of myocardial infarction, that the survival is dramatically decreased in $NOS1^{-/-}$ mice (40). Interestingly, it has been described that pharmacological blockade of NOS1 increases ventricular fibrillation in models of ischemia–reperfusion, in a manner that is reversed by NO donors (41–43).

It is known that NOS1 is up-regulated after myocardial infarction and is redistributed from the SR to the plasmalemma (2, 7, 44). This translocation may inhibit the Ca^{2+} influx from the plasma membrane but, at the same time, disrupt the Ca^{2+} storage in the SR as we show here. Furthermore, this disruption in Ca^{2+} homeostasis is closely linked to ventricular tachycardia, arrhythmias, and sudden cardiac death (45, 46). Similarly, increased *S*-nitrosylation of the α_{1c} subunit of the L-type calcium channel is observed in patients with atrial fibrillation (47), in this case associated with a decreased calcium influx.

There is a limitation to our work: it has to be noted that in our assessment of Ca^{2+} leak, the load–leak function appears somehow different from what was originally described (a more exponential behavior). Although it was not our intent in this work to examine the nonlinearity of the load–leak relationship, the dependence of the leak on the SR load in our work compared with the exponential appearance reported in the rabbit (11, 48) would suggest that RyR open probability may be more constant over the range of loads in our work. Although this observation is potentially explainable by the nitroso–redox modulation of the RyR and its alteration in the NOS1-deficient mice, a future study is required to assess this issue.

In summary, NOS1 deficiency causes diminished RyR2 *S*-nitrosylation and increased oxidation, which in turn lead to increased diastolic Ca^{2+} and reduced intra-SR Ca^{2+} content. This leakage, in turn, decreased contractility and increased electrical instability, key features of heart failure. Together, these findings establish the importance of endogenous RyR2 *S*-nitrosylation mediated by NOS1 and provide mechanistic insights whereby NOS1 deficiency may lead to depressed myocardial contractility as well as to sudden cardiac death.

Materials and Methods

Animals. We studied transgenic mice (males and females, 3–6 months old) with homozygous deletions of NOS1 (49), NOS3 (50), and double NOS1/NOS3 knockout (51) bred on a C57BL/6 background that was used as WT (Jackson Laboratories). All protocols and experimental procedures were approved by the Animal Care and Use Committee of the Johns Hopkins University School of Medicine and the Miller School of Medicine.

Isolation of Myocytes. Please see *SI Methods*.

Sarcomere length (SL) and Ca^{2+} transients ($[Ca^{2+}]_i$) were measured in myocytes stimulated at 1, 2, 4, 6, and 8 Hz. All experiments were conducted at 37°C.

SL was recorded with an IonOptix iCCD camera. Changes in average SL were determined by fast Fourier transform of the *Z*-line density trace to the frequency domain, and SL shortening was calculated as follows:

$$\text{shortening} = (\text{diastolic SL} - \text{systolic SL})/\text{diastolic SL}. \quad [1]$$

Assessment of SR Ca^{2+} Leak. Calcium leak was assessed as described by Shannon *et al.* (11). Ventricular myocytes were loaded with fura-2 and paced by field stimulation at the different frequencies in normal Tyrode until cellular Ca^{2+} transients reached a steady state. After the last pulse, the superfusing solution was rapidly switched to 0 Na^+/0 Ca^{2+} (Na^+ replaced by Li^+) Tyrode. In the control condition, $[Ca^{2+}]_i$ was monitored while 0 Na^+/0 Ca^{2+} Tyrode buffer was applied for at least 40 s to eliminate transsarcolemmal Ca^{2+} fluxes, creating a closed system with a steady-state $[Ca^{2+}]_i$. Then a rapid pulse of 10 mM caffeine was added to cause SR Ca^{2+} release. After the cell recovered, it was stimulated again in the same conditions, but the 0 Na^+/0 Ca^{2+} Tyrode solution contained 1 mM tetracaine. Under this condition, RyR is inhibited, and the shift (decrease) in the fura signal (cytosolic $[Ca^{2+}]$) is observed. In this condition, the leak is blocked, and the difference in $[Ca^{2+}]_T$ between tetracaine and control condition corresponds to diastolic leak. The amplitude of the caffeine-induced Ca^{2+} transient was used to estimate the total $[Ca^{2+}]_i$. To calculate $[Ca^{2+}]_T$ in the SR, the amplitude of the caffeine-induced transient was converted to total SR Ca content considering the cell volume as 33 pl (52), 3% of it being the SR and 65% the volume of the cytosol (11). Subsequently, the load–leak relationship was constructed plotting the total SR Ca load versus the diastolic leak at the different frequencies of stimulation.

$[Ca^{2+}]_i$ Calibration. The signal of fura-2 was measured as a ratio of the fluorescence at 365/380 nm. This signal was converted to $[Ca^{2+}]_i$ with the method described by Grynkiewicz *et al.* (53), using the function:

$$[Ca^{2+}]_i = K_d(F - F_{min})/(F_{max} - F), \quad [2]$$

where K_d is the dissociation constant for fura-2 at 35°C, F is the ratio of the fluorescence at 365/380 of the fluorescence, F_{min} is the minimal signal at 0 Ca^{2+} conditions, and F_{max} is the value obtained at saturating Ca^{2+} conditions, both using permeabilized cardiomyocytes with ionomycin.

Assessment of *S*-Nitrosylation. For determination of RyR nitrosylation, hearts were treated as above, and the biotin switch technique was performed accordingly to Jaffrey *et al.* (54, 55). For details, see *SI Methods*.

Free Thiols Assessment. Free thiols in the RyR were assessed by using the fluorescent probe for cysteines monobromobimane (56) (Calbiochem) as described (3, 32, 57) with some modifications. Total heart homogenates were incubated with 1 mM monobromobimane for 1 h at room temperature in the dark. The reaction was stopped with 1 mM L-cysteine. Proteins were resolved in 3–8% Tris acetate gels and transilluminated with UV light. Total RyR2 was identified upon silver staining of the gel and confirmed by Western blotting with anti-RyR and by mass spectrometry (data not shown). Free cysteines content is expressed as the ratio of the optical density of the UV signal to the total RyR signal (silver staining).

Statistical Analysis. Data are expressed as mean ± SEM. For comparisons of two groups, an unpaired two-tailed Student's t test was used. For comparison of more than three groups, ANOVA (one- or two-way as appropriate) was performed with the Bonferroni post hoc test. For all tests, $P < 0.05$ was considered significant.

ACKNOWLEDGMENTS. This work was supported by National Institutes of Health Grant R01 HL-65455.

1. Barouch LA, Harrison RW, Skaf MW, Rosas GO, Cappola TP, Kobeissi ZA, Hobai IA, Lemmon CA, Burnett AL, O'Rourke B, *et al.* (2002) *Nature* 416:337–339.
2. Damy T, Ratajczak P, Shah AM, Camors E, Marty I, Hasenfuss G, Marotte F, Samuel JL, Heymes C (2004) *Lancet* 363:1365–1367.
3. Xu L, Eu JP, Meissner G, Stamler JS (1998) *Science* 279:234–237.
4. Schuh K, Uldrijan S, Telkamp M, Rothlein N, Neyses L (2001) *J Cell Biol* 155:201–205.
5. Burkard N, Rokita AG, Kaufmann SG, Hallhuber M, Wu R, Hu K, Hofmann U, Bonz A, Frantz S, Cartwright EJ, *et al.* (2007) *Circ Res* 100:e32–e44.
6. Casadei B (2006) *Exp Physiol* 91:943–955.
7. Damy T, Ratajczak P, Robidel E, Bendall JK, Oliviero P, Boczkowski J, Ebrahimian T, Marotte F, Samuel JL, Heymes C (2003) *FASEB J* 17:1934–1936.
8. Sun J, Picht E, Ginsburg KS, Bers DM, Steenbergen C, Murphy E (2006) *Circ Res* 98:403–411.
9. Khan SA, Skaf MW, Harrison RW, Lee K, Minhas KM, Kumar A, Fradley M, Shoukas AA, Berkowitz DE, Hare JM (2003) *Circ Res* 92:1322–1329.
10. Khan SA, Lee K, Minhas KM, Gonzalez DR, Raju SV, Tejani AD, Li D, Berkowitz DE, Hare JM (2004) *Proc Natl Acad Sci USA* 101:15944–15948.
11. Shannon TR, Ginsburg KS, Bers DM (2002) *Circ Res* 91:594–600.
12. Venetucci LA, Trafford AW, Diaz ME, O'Neill SC, Eisner DA (2006) *Circ Res* 98:1299–1305.
13. Babu BR, Griffith OW (1998) *J Biol Chem* 273:8882–8889.
14. Sears CE, Bryant SM, Ashley EA, Lygate CA, Rakovic S, Wallis HL, Neubauer S, Terrar DA, Casadei B (2003) *Circ Res* 92:e52–e59.
15. Wehrens XH, Marks AR (2003) *Trends Biochem Sci* 28:671–678.
16. Wehrens XH, Lehnart SE, Reiken S, Vest JA, Wronska A, Marks AR (2006) *Proc Natl Acad Sci USA* 103:511–518.
17. Negretti N, O'Neill SC, Eisner DA (1993) *Cardiovasc Res* 27:1826–1830.
18. Rubart M, Zipes DP (2005) *J Clin Invest* 115:2305–2315.
19. Aracena P, Sanchez G, Donoso P, Hamilton SL, Hidalgo C (2003) *J Biol Chem* 278:42927–42935.
20. Eu JP, Sun J, Xu L, Stamler JS, Meissner G (2000) *Cell* 102:499–509.
21. Sun J, Xin C, Eu JP, Stamler JS, Meissner G (2001) *Proc Natl Acad Sci USA* 98:11158–11162.
22. Sun J, Xu L, Eu JP, Stamler JS, Meissner G (2001) *J Biol Chem* 276:15625–15630.
23. Saraiva RM, Minhas KM, Zheng M, Pitz E, Treuer A, Gonzalez D, Schuleri KH, Vandegaer KM, Barouch LA, Hare JM (2007) *Nitric Oxide* 16:331–338.
24. Xu KY, Huso DL, Dawson TM, Bredt DS, Becker LC (1999) *Proc Natl Acad Sci USA* 96:657–662.
25. Dedkova EN, Wang YG, Ji X, Blatter LA, Samarel AM, Lipsius SL (2007) *J Physiol (London)* 580:327–345.
26. Ter Keurs HE, Boyden PA (2007) *Physiol Rev* 87:457–506.
27. Liu N, Colombi B, Memmi M, Zissimopoulos S, Rizzi N, Negri S, Imbriani M, Napolitano C, Lai FA, Priori SG (2006) *Circ Res* 99:292–298.
28. Knollmann BC, Chopra N, Hlaing T, Akin B, Yang T, Ettensohn K, Knollmann BE, Horton KD, Weissman NJ, Holinstat I, *et al.* (2006) *J Clin Invest* 116:2510–2520.
29. Yuan Q, Fan GC, Dong M, Altschafl B, Diwan A, Ren X, Hahn HH, Zhao W, Waggoner JR, Jones LR, *et al.* (2007) *Circulation* 115:300–309.
30. Wehrens XH, Lehnart SE, Huang F, Vest JA, Reiken SR, Mohler PJ, Sun J, Guatimosim S, Song LS, Rosemblit N, *et al.* (2003) *Cell* 113:829–840.
31. Kinugawa S, Huang H, Wang Z, Kaminski PM, Wolin MS, Hintze TH (2005) *Circ Res* 96:355–362.
32. Yano M, Okuda S, Oda T, Tokuhisa T, Tateishi H, Mochizuki M, Noma T, Doi M, Kobayashi S, Yamamoto T, *et al.* (2005) *Circulation* 112:3633–3643.
33. Aghdasi B, Reid MB, Hamilton SL (1997) *J Biol Chem* 272:25462–25467.
34. Zahradnikova A, Minarovic I, Venema RC, Meszaros LG (1997) *Cell Calcium* 22:447–454.
35. Hart JD, Dulhunty AF (2000) *J Membr Biol* 173:227–236.
36. Suko J, Drobny H, Hellmann G (1999) *Biochim Biophys Acta* 1451:271–287.
37. Kubalova Z, Terentyev D, Viatchenko-Karpinski S, Nishijima Y, Gyorke I, Terentyeva R, da Cunha DN, Sridhar A, Feldman DS, Hamlin RL, *et al.* (2005) *Proc Natl Acad Sci USA* 102:14104–14109.
38. Marengo JJ, Hidalgo C, Bull R (1998) *Biophys J* 74:1263–1277.
39. Barouch LA, Cappola TP, Harrison RW, Crone JK, Rodriguez ER, Burnett AL, Hare JM (2003) *J Mol Cell Cardiol* 35:637–644.
40. Saraiva RM, Minhas KM, Raju SV, Barouch LA, Pitz E, Schuleri KH, Vandegaer K, Li D, Hare JM (2005) *Circulation* 112:3415–3422.
41. Kumar K, Nguyen K, Waxman S, Nearing BD, Wellenius GA, Zhao SX, Verrier RL (2003) *J Am Coll Cardiol* 41:1831–1837.
42. Pabla R, Curtis MJ (1995) *Circ Res* 77:984–992.
43. Pabla R, Curtis MJ (1996) *J Mol Cell Cardiol* 28:2097–2110.
44. Bendall JK, Damy T, Ratajczak P, Loyer X, Monceau V, Marty I, Milliez P, Robidel E, Marotte F, Samuel JL, *et al.* (2004) *Circulation* 110:2368–2375.
45. Kannankeril PJ, Mitchell BM, Goonasekera SA, Chelu MG, Zhang W, Sood S, Kearney DL, Danila CI, De BM, Wehrens XH, *et al.* (2006) *Proc Natl Acad Sci USA* 103:12179–12184.
46. Paavola J, Viitasalo M, Laitinen-Forsblom PJ, Pasternack M, Swan H, Tikkanen I, Toivonen L, Kontula K, Laine M (2007) *Eur Heart J* 28:1135–1142.
47. Carnes CA, Janssen PM, Ruehr ML, Nakayama H, Nakayama T, Haase H, Bauer JA, Chung MK, Fearon IM, Gillinov AM, *et al.* (2007) *J Biol Chem* 282:28063–28073.
48. Shannon TR, Pogwizd SM, Bers DM (2003) *Circ Res* 93:592–594.
49. Huang PL, Dawson TM, Bredt DS, Snyder SH, Fishman MC (1993) *Cell* 75:1273–1286.
50. Huang PL, Huang Z, Mashimo H, Bloch KD, Moskowitz MA, Bevan JA, Fishman MC (1995) *Nature* 377:239–242.
51. Son H, Hawkins RD, Martin K, Kiebler M, Huang PL, Fishman MC, Kandel ER (1996) *Cell* 87:1015–1023.
52. Shannon TR, Wang F, Puglisi J, Weber C, Bers DM (2004) *Biophys J* 87:3351–3371.
53. Grynkiewicz G, Poenie M, Tsien RY (1985) *J Biol Chem* 260:3440–3450.
54. Jaffrey SR, Snyder SH (2001) *Sci STKE* 2001:PL1.
55. Jaffrey SR, Erdjument-Bromage H, Ferris CD, Tempst P, Snyder SH (2001) *Nat Cell Biol* 3:193–197.
56. Kosower NS, Kosower EM (1987) *Methods Enzymol* 143:76–84.
57. Yano M, Yamamoto T, Ikemoto N, Matsuzaki M (2005) *Pharmacol Ther* 107:377–391.